March 2007

Piezomagnetism in epitaxial Cr2O3 thin films and spintronic applications

Sarbeswar Sahoo
sarbeswar@gmail.com

Christian Binek
cbinek@unl.edu

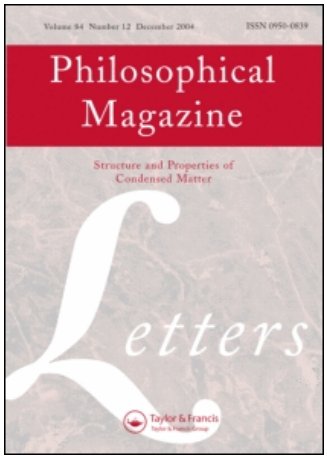

Philosophical Magazine Letters
Publication details, including instructions for authors and subscription information:
http://www.informaworld.com/smpp/title~content=t713695410

Piezomagnetism in epitaxial Cr_2O_3 thin films and spintronic applications

To cite this Article: , 'Piezomagnetism in epitaxial Cr_2O_3 thin films and spintronic applications', Philosophical Magazine Letters, 87:3, 259 - 268
xxxx:journal To link to this article: DOI: 10.1080/09500830701253177
URL: http://dx.doi.org/10.1080/09500830701253177

Philosophical Magazine Letters,
Vol. 87, Nos. 3–4, March–April 2007, 259–268

Piezomagnetism in epitaxial Cr_2O_3 thin films and spintronic applications

S. SAHOO and CH. BINEK*

Department of Physics and Astronomy and the Nebraska Center for Materials and Nanoscience, University of Nebraska-Lincoln, 203 Ferguson Hall, NE 68588-0111, USA

(*Received 10 November 2006; accepted in revised form 23 January 2007*)

Stress-induced perturbation of the antiferromagnetic long-range order in epitaxially grown (111) Cr_2O_3 thin films gives rise to pronounced piezomagnetism and a significant reduction of the antiferromagnetic ordering temperature. The temperature dependence of the piezomagnetic moment measured by superconducting quantum interference device magnetometry reveals a power law behaviour with a critical exponent $2\beta = 0.66$ in accordance with the Ising anisotropy of a three-dimensional system. The observed shift of the Néel temperature allows estimating the internal lateral stress which is in excellent agreement with an independent estimate based on the elastic properties of Cr_2O_3 and the lattice mismatch at the interface between the sapphire substrate and the isostructural (111) Cr_2O_3 thin film. The isothermal freezing field dependence of the piezomoment is interpreted in terms of Zeeman energy arguments. Implications of the piezomagnetic effects for spintronic devices and the investigation of the piezomagnetoelectric effect are briefly discussed.

1. Introduction

In magnetoelectric (ME) materials a linear magnetic response M^i (electric response P^i) can be induced by the application of an electric field E_j (magnetic field H_j) such that $M^i = \alpha^{ij}_{me} E_j$ and $P^i = \alpha^{ij}_{em} H_j$, where $\alpha^{ij}_{me} = \alpha^{ji}_{em}$ are the tensors of ME susceptibility and its transpose counterpart and i, j label the vector and tensor components, respectively [1, 2]. These materials offer novel approaches to realize a new generation of spintronic devices [3]. Currently, there is growing scientific interest to explore the ME effect in magnetic ferroelectrics where polarization spontaneously occurs [4–6]. Among them are the multiferroic systems which exhibit a coexistence of spontaneous ferromagnetic and ferroelectric order. Coupling between the ferroic order parameters can give rise to a pronounced ME response [7]. It is expected that a variety of spectacular applications are likely to emerge, in particular in the field of non-volatile data storage, if ultimately reversal of one order parameter is achieved by applying the conjugate field of its coexisting counterpart. Despite the recent progress in the field of multiferroics, huge ME effects are still rare exceptions rather than the rule, while the potential which

*Corresponding author. Email: cbinek2@unl.edu

Philosophical Magazine Letters
ISSN 0950-0839 print/ISSN 1362-3036 online © 2007 Taylor & Francis
http://www.tandf.co.uk/journals
DOI: 10.1080/09500830701253177

classical ME compounds like Cr_2O_3 provide for spintronic applications is still far from being fully explored. We therefore focus here on epitaxially grown ME Cr_2O_3 thin films which resemble an important step towards recently suggested spintronic applications [3].

Whereas ME effects refer to electrically induced magnetization, we report here on a pronounced stress-induced magnetization known as the piezomagnetic effect [8]. The coexistence of the ME effect and piezomagnetism and the potential to observe their coupling via the piezomagnetoelectric effect [9] make such films particularly attractive. Piezoelectrically controlled piezomagnetism for instance provides an alternative route towards the realization of various spintronic applications. Piezomagnetism is a well known but weak phenomenon in many bulk antiferromagnetic (AF) materials. It is described by a third rank tensor P_{ikl} which is usually defined by $M_i = P_{ikl}\sigma_{kl}$, where M_i is the magnetic moment developed in direction i and σ_{kl} is the applied stress. In this letter we deal with the prototypical ME compound, Cr_2O_3 [10–12], on the nanometre scale. We study its epitaxial growth, perform detailed structural analysis and present for the first time the observation of a pronounced piezomagnetic effect.

Bulk Cr_2O_3 has a close-packed corundum structure ($a = 4.958$ Å, $c = 13.594$ Å) with rhombohedral symmetry. (111) planes containing the Cr^{3+} ions in a zigzag arrangement have to be considered as uncompensated ferromagnetic planes when interface roughness is neglected. Cr_2O_3 belongs to the magnetic point group $\bar{3}'m'$ and undergoes an AF transition below the Néel temperature, $T_N = 307$ K and exhibits a uniaxial magnetic anisotropy along [111]. Not only do its AF properties make it useful as a pinning layer in exchange bias (EB) systems but its insulating and ME properties open additional possibilities as an active tunnelling barrier or pinning system for spintronic applications. More specifically, one can consider an electrical field control of the magnetization states in giant magnetoresistance (GMR) or tunnel magnetoresistance (TMR) structures which can provide an alternative to current-induced switching mechanisms [3]. So far, prototypical Cr_2O_3(111)/CoPt heterostructures have been realized only on the basis of (111) oriented Cr_2O_3 bulk single crystals [13, 14]. In order to fabricate spintronic devices, such as those proposed by Binek and Doudin [3], highest quality Cr_2O_3 (111) thin films have to be grown in proximity of metallic thin films.

2. Preparation of Cr_2O_3 thin films

Since Cr exhibits multiple oxide states (+3, +4, +6), previous studies reveal that stringent control of the oxygen partial pressure and substrate temperature during the evaporation of Cr metal has to be fulfilled in order to optimize the growth of stoichiometric Cr_2O_3 films [15]. The molecular beam epitaxy (MBE) growth technique at a chamber base pressure of 5×10^{-11} mbar was used. Single crystalline Cr_2O_3 (111) films were grown on c-plane Al_2O_3 substrate by thermal evaporation of Cr metal from a Knudsen cell in an O_2 background pressure of 2.2×10^{-6} mbar. The substrate temperature was maintained at 300°C. For this growth kinetics,

the growth rate of Cr_2O_3 films monitored by a calibrated quartz oscillator was found to be $0.28\,nm\,min^{-1}$.

3. Structural characterization

We employed various configurations of an X-ray analysis station (Bruker AXS-D8 Discover) to perform detailed structural characterization of Cr_2O_3 thin films. Figure 1a shows the parallel beam X-ray diffraction (XRD) pattern of Cr_2O_3 film grown on *c*-plane Al_2O_3 substrate. Analysis of these data by using rhombohedral unit cell parameters confirms (111)-oriented single crystalline epitaxial growth of the Cr_2O_3 film.

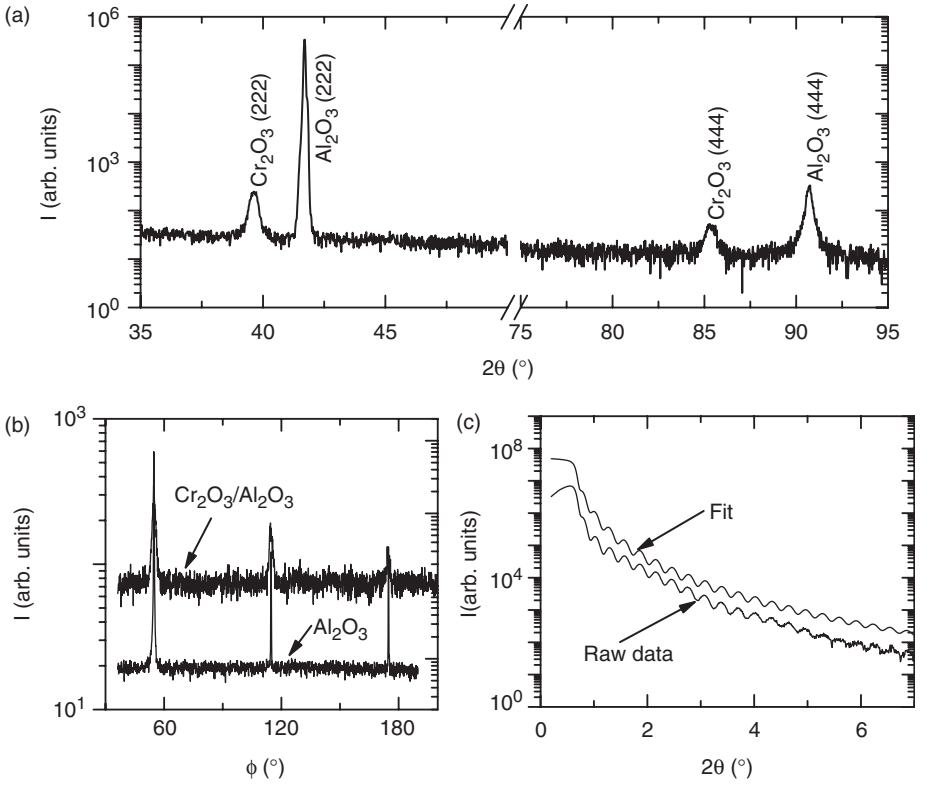

Figure 1. (a) High resolution X-ray diffraction pattern of Cr_2O_3 thin film grown on *c*-plane Al_2O_3 substrate. Note the break in the X-axis. (b) Φ scans with *k* fixed to the orthorhombic (110) reflection. Upper pattern represents the scan taken on the Cr_2O_3 film, whereas the lower pattern represents the scan on the bare Al_2O_3 substrate. In both cases the reflections are separated by 60°, indicating sixfold in-plane symmetry. (c) Small-angle X-ray reflection curve of Cr_2O_3 film. The upper curve is the best fit by using LEPTOS-2 program to the lower raw data. In (b) and (c) the curves are mutually shifted along the intensity axis for clearer presentation.

In order to examine the in-plane structural symmetry of Cr_2O_3 films we used in-plane grazing incidence X-ray diffraction (Φ scans). In this technique the X-ray beam is incident on the sample plane at a grazing angle less than the critical angle of total reflection. This induces evanescent waves parallel to the sample surface which excite Bragg reflections from atomic planes perpendicular to the surface. Figure 1b shows a comparison of the intensity of Bragg peaks for an Al_2O_3/Cr_2O_3 film (upper pattern) and an Al_2O_3 substrate (lower pattern) as a function of sample rotation angle Φ from 0° to 180°. The scattering vector k is kept constant at the bulk orthorhombic Cr_2O_3 (110) Bragg peak and the sample is rotated around the Φ axis oriented normal to the surface. The epitaxial relationship of the film with the substrate is clearly evidenced from the observed three peaks separated by 60° in both cases indicating sixfold (hexagonal) symmetry in the plane. Variation of the peak intensities arises from the slight misalignment of sample plane with respect to the incident beam.

Figure 1c shows the small angle X-ray reflectometry (SAXR) curve of an Al_2O_3/Cr_2O_3 film (lower curve) and the best fit by using LEPTOS-2 software (upper curve). Periodic oscillations corresponding to Bragg peaks are resolved up to 20th order. Analysis of the fit yields a total thickness of the film of 28 nm and mean values of interface and surface roughness as 0.1 nm and 0.3 nm, respectively. This is consistent with the thickness expected from the growth rate monitored by the quartz oscillator.

4. Magnetic characterization

Magnetization measurements were carried out by the use of a commercial superconducting quantum interference device (SQUID) magnetometer (Quantum Design MPMS-XL) following different experimental protocols. For zero-field cooled field-heated measurements of the magnetic moment, $m^{\text{ZFC-FH}}$, the sample was cooled in virtual zero field from $T = 395\,\text{K} > T_N$ to $T < T_N$, where a field step $\mu_0 H$ was applied along the [111] direction. Subsequently $m^{\text{ZFC-FH}}$ vs. T was measured on heating. Note that true zero-field cooling conditions have not been achieved due to residual magnetic flux trapped in the superconducting solenoid. The field-cooled magnetic moment, m^{FC}, was measured upon cooling from $T = 395\,\text{K}$ to $T < T_N$ in the presence of the axial applied magnetic field. The subsequent heating in the same field is called field-cooled field–heated magnetic moment, $m^{\text{FC-FH}}$. The thermoremnant moment, m^{TRM}, is prepared by cooling the sample from $T = 395\,\text{K}$ in a constant field to $T < T_N$. Subsequently, m^{TRM} vs. T is measured on heating in zero magnetic field.

Figure 2 shows representative $m^{\text{ZFC-FH}}$, m^{FC}, $m^{\text{FC-FH}}$ and m^{TRM} vs. T curves of Cr_2O_3 (28 nm)/Al_2O_3 sample involving a small magnetic field, $\mu_0 H = 1\,\text{mT}$ in the preparation procedures described above. All data sets differ drastically from the regular AF bulk behaviour where the magnetization freezes out with decreasing temperature to $T < T_N$ due to compensating sublattice magnetization. Above T_N in bulk Cr_2O_3, the field induced magnetization decays according to a Curie–Weiss type behaviour $M \propto 1/(T-\theta)$ where $\theta \approx -360\,\text{K}$. Here, however, we measure an increasing magnetization with decreasing temperature at $T < T_N$. Instead of the

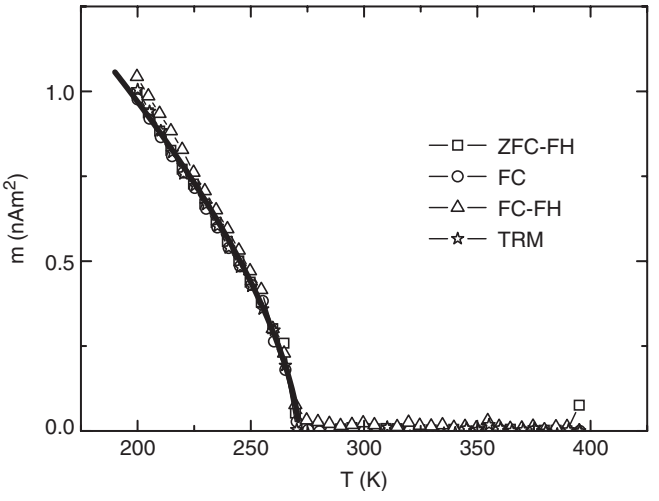

Figure 2. Temperature variation of $m^{\mathrm{ZFC\text{-}FH}}$ (squares), m^{FC} (circles), $m^{\mathrm{FC\text{-}FH}}$ (triangles) and m^{TRM} (stars) involving a magnetic field of $\mu_0 H = 1\,\mathrm{mT}$. The solid line represents the best fit according to equation (1).

typical AF fingerprints, our data indicate that a piezomoment is imprinted during the freezing process. This applies also to the $m^{\mathrm{ZFC\text{-}FH}}$ vs. T curve due to the presence of a residual field as mentioned above. Once frozen, moderate variation of the magnetic field leaves the piezomoment invariant. Our subsequent analysis rules out the possibility that the observed moment arises from an uncompensated surface spin layer where two-dimensional (2D) behaviour might be expected. We attribute the observed moment to the piezomagnetic effect where the sublattice degeneracy is lifted by stress. The latter is induced via the interface lattice mismatch between the c-plane of the sapphire substrate and the Cr_2O_3 film. The temperature dependence of the piezomoment follows the 3D Ising order parameter behaviour according to

$$m = m_0 \left(1 - \frac{T}{T_{\mathrm{N}}}\right)^{2\beta}. \tag{1}$$

The exponent 2β in equation (1) indicates that the piezomagnetism in Cr_2O_3 originates from the stress dependence of the crystal field tensor [16]. The best fit of equation (1) to $m^{\mathrm{ZFC\text{-}FH}}$ data yields the reduced thin film Néel temperature, $T_{\mathrm{N}} = 271 \pm 1\,\mathrm{K}$ and the critical exponent, $2\beta = 0.66 \pm 0.01$ in perfect agreement with 3D Ising criticality. We observe a significant shift in T_{N} from the bulk value $T_{\mathrm{N}} = 307\,\mathrm{K}$ by $\Delta T_{\mathrm{N}} = 36\,\mathrm{K}$. This value indicates on the one hand that the lengths and angles of the superexchange paths are changed and on the other hand allows estimating the magnitude of the lateral stress according to $\sigma = |\Delta\sigma/\Delta T_{\mathrm{N}}|\Delta T_{\mathrm{N}} \approx 6.0 \times 10^9\,\mathrm{Pa}$, where the bulk value $|\Delta\sigma/\Delta T_{\mathrm{N}}| = 1.66 \times 10^8\,\mathrm{Pa\,K^{-1}}$ was used [17, 18]. Alternatively, considering the lattice mismatch, $\varepsilon = 4\%$, between the bulk rhombohedral unit cells of Al_2O_3 and Cr_2O_3 we estimated the induced stress according to $\sigma = C\varepsilon \approx 4.0 \times 10^9\,\mathrm{Pa}$, where $C \approx 10^{11}\,\mathrm{Pa}$ [19]. Both approaches are in good qualitative agreement. Note, however, that the data reported by

Gorodetsky *et al.* [17] suggest an increase in T_N with increasing uniaxial and hydrostatic pressure, whereas earlier results [18] obtained by time of flight neutron diffraction evidence the opposite sign but virtually the same magnitude in the pressure dependence of T_N. This apparent contradiction has been stressed by Gorodetsky *et al.* [17] although its origin remains unclear. Our results on Cr_2O_3 thin films show that compressive strain reduces T_N in accordance with the early neutron data of Worlton *et al.* [18]. Here, AF long-range correlation is directly probed via the temperature dependence of the scattering intensity of the (110) peak. In contrast, the magnetoelectric approach presented by Gorodetsky *et al.* [17] is indirect in the sense that the pressure dependence of T_N is deduced via the pressure and temperature dependence of various elements of the magnetoelectric susceptibility tensor, α_{me}^{ij}, which is still poorly understood. The early phenomenological approach by Rado [12] implied $\alpha_{me}^{ij} \propto \chi^{ij}\langle S_z\rangle$, where χ^{ij} is the magnetic susceptibility and $\langle S_z\rangle$ is the AF sublattice magnetization. This intuitive expression fails in describing basic features of the α_{me}^{ij} vs. T behaviour such as the change of the sign of α_{me}^{ij} at $T \approx 100\,\mathrm{K}$ [12]. The latter has its microscopic origin in the interplay between T-dependent single-ion and two-ion terms. The single-ion term resembles the electric field dependence of the Landé g-tensor and the single-ion anisotropy while the two-ion term describes the electric field dependence of Cr^{3+} superexchange involved in α_{me}^{zz}. Advanced thermodynamic considerations [20] show that the relation between α_{me}^{ij} and $\langle S_z\rangle$ is by far more involved than Rado's simple proportionality suggests. Therefore one should not expect that T_N can be deduced from α_{me}^{ij} vs. T data in particular in the presence of applied pressure where a detailed thermodynamic theory is lacking. However, similar to neutron diffraction the piezomagnetic moment is related to the sublattice magnetization. Hence, our finding of reduced T_N in the presence of compressive misfit strain is in agreement with the original neutron experiments of Worlton *et al.* [18].

Figure 3a shows the temperature variation of m^{TRM} at $1 \le \mu_0 H \le 50\,\mathrm{mT}$. The magnitude of m^{TRM} increases with applied freezing field $\mu_0 H$, but approaches saturation at $\mu_0 H \ge 20\,\mathrm{mT}$. Analysis of these data after subtracting the respective linear background contribution (line in figure 3a) indicates that m^{TRM} vs. T curves differ by a scale factor only. Thus each curve normalized by the moment at an arbitrary but fixed reference temperature $T_r < T_N$ reveals a data collapse onto a single master curve. Figure 3b shows the result of our scaling analysis obtained from the eight data sets in figure 3a after normalization with $m_r = m(T = 200\,\mathrm{K})$. The scaling behaviour resembles the fact that the piezomoment $m = m(H, T)$ factorizes according to $m(H, T) = f(H)\ g(T)$ where f and g are functions of field and temperature, respectively. Normalizing the various $m(H, T)$ curves by the respective magnetic moment $m(H, T_r)$ at $T_r < T_N$ yields the universal behaviour $m(H, T)/m(H, T_r) = g(T)/g(T_r)$.

The product functional form of $m(H, T)$ is a consequence of the field selected orientation of the local piezomoment. A magnetic field favours parallel orientation of the piezomoment which develops on cooling. In the case of single domain AF order, the local piezomoment follows the lateral stress distribution. In an applied magnetic field, however, the piezomoment favours parallel alignment in order to minimize the Zeeman energy. This process imprints an AF multi domain state [21].

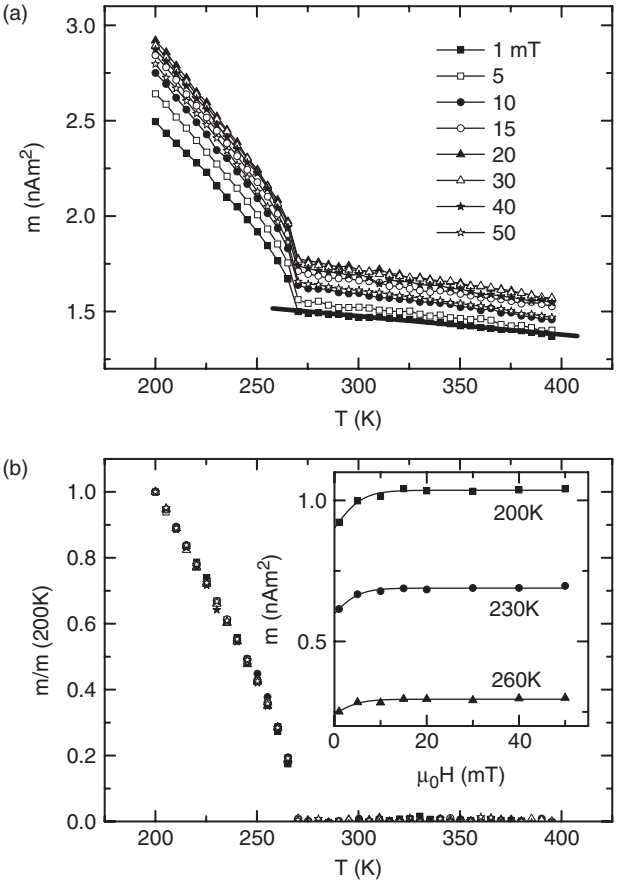

Figure 3. (a) m^{TRM} vs. T at various magnetic fields as indicated. The solid line shows the background subtraction. (b) Scaling plot of the normalized magnetization m/m (200 K) vs. T. Inset shows m vs. H isotherms at $T = 200$, 230 and 260 K. The lines are the best fits to a functional form $m = \hat{m} \tanh \mu\mu_0 H/k_B T$.

Figure 4 shows $m^{\mathrm{FC\text{-}FH}}$ and m^{FC} vs. T after cooling through T_{N} in the presence of an axial magnetic field $\mu_0 H = -5$ mT, whereas subsequent measurements take place in a positive field of $\mu_0 H = 5$ mT. A sketch of the experimental procedure is shown in the inset to figure 4. Nearly perfect inversion symmetry of both curves evidences the field selection of the orientation of the piezomoment. Note that once the system is frozen in below T_{N} moderate changes of the applied magnetic field have no impact on the temperature dependence of m. This behaviour indicates that the piezomoment is correlated with an imprinted AF domain structure whose rearrangement is energetically highly unfavourable.

The inset of figure 3b shows m vs. H isotherms at $T = 200$, 230 and 260 K, respectively. They are obtained from an isothermal cross-section of m^{TRM} vs. T data of figure 3a after background correction. The isotherms hint at a large spontaneous background which in turn indicates that the lateral stress distribution $\sigma = \sigma(\underline{r})$ has a non-zero spatial average $\langle \sigma(\underline{r}) \rangle < 0$ creating a net in-plane compression. This net

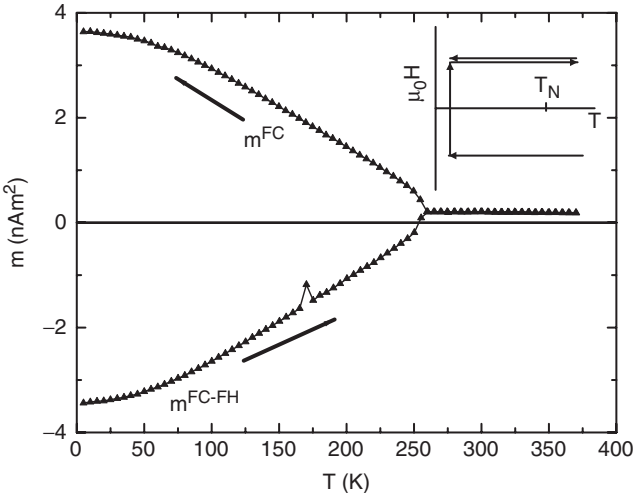

Figure 4. $m^{\mathrm{ZFC\text{-}FH}}$ and $m^{\mathrm{FC\text{-}FH}}$ vs. T following the experimental protocol sketched in the inset.

compression selects one of the AF 180° domains via minimization of the Zeeman energy. The latter is determined by the piezomoment aligned parallel to the freezing field applied on cooling to below T_N. In the case of moderate freezing fields $\mu_0 H < 15\mathrm{mT}$ the piezomoment is not fully saturated which means that local contributions point in opposite direction to the average moment. The parallel reorientation of these regions can be energetically driven when increasing the strength of the freezing field. Quantitatively, this control takes place via Boltzmann factors involving the Zeeman energy of these local piezomoments, μ, adding up to a saturation value, $\hat{m}$. This statistical approach gives rise to a functional form $m = \hat{m} \tanh \mu\mu_0 H/k_B T$, as represented by lines in the inset of figure 3b.

5. Spintronic applications and opportunities for basic research

The coexistence of magnetoelectric, piezomagnetic and perhaps piezomagnetoelectric characteristics and a stress induced T_N shift make Cr_2O_3 thin films a promising component for future spintronic applications. ME spintronic devices such as those proposed by Binek and Doudin [3] depend on highest quality Cr_2O_3 films.

Based on the findings presented here, additional extrinsic control of stress in Cr_2O_3 thin film based EB systems [13, 14] will allow for (piezo)electrically controlled spin valve architectures for instance. This has the potential to become an alternative to the electrically controlled EB based on ME pinning layers suggested previously [3]. Similarly, one can think about stress induced switching of the AF order in Cr_2O_3 pinning layers where the bias field in an EB system can be switched on and off by switching the AF order. The control of the stress can be achieved by piezoelectric substrates or substrates undergoing temperature induced structural changes.

In addition, as pointed out above AF single and multi domain states can be prepared which minimize and maximize the piezomoment. Since the latter will contribute to the interface magnetization we can tune exchange bias with an adjacent FM film by switching the piezomoment on or off. This additional controllable interface moment is expected to enhance the recently observed ME switching effect [13].

Finally, the magnetic point group symmetry of Cr_2O_3 allows for the piezomagnetoelectric effect. The high inherent stress, a significant piezomagnetic moment and the possibility to realize high electric fields makes Cr_2O_3 thin films ideal candidates for the challenging quest of the symmetry allowed but hitherto undiscovered piezomagnetoelectric effect [9].

6. Conclusion

In conclusion, we have shown that epitaxially grown crystalline Cr_2O_3 thin films exhibit an unusually large piezomagnetic effect. The intrinsic stress reduces the AF bulk Néel temperature, T_N, by 36 K for our Cr_2O_3 film of thickness 28 nm. The local orientation of the piezomagnetic moment determines the sign of the local AF order parameter via the stress distribution in the sample. The field selected piezomoment follows a power law behaviour at T_N with an exponent $2\beta = 0.66$ of the 3D Ising system. We propose that the pronounced piezomagnetic effect observed in our Cr_2O_3 thin films and its inherent magnetoelectric characteristics can be exploited in potential device applications as well as in the investigation of new physical phenomena like the piezomagnetoelectric effect.

Acknowledgements

Financial support from the NSF through Career DMR-0547887, Nebraska Research Initiative (NRI) and the MRSEC Program of the NSF (DMR-0213808) is gratefully acknowledged.

References

[1] P. Curie, J. Phys., Paris, III **3** 393 (1894).
[2] I. E. Dzyaloshinskii, Soviet Phys. JETP **10** 628 (1960).
[3] C. Binek and B. Doudin, J. Phys. Condens. Matt. **17** L39 (2005).
[4] M. Fiebig, J. Phys. D **38** R123 (2005).
[5] W. Eerenstein, N. D. Mathur and J. F. Scott, Nature **442** 759 (2006).
[6] E. Y. Tsymbal and H. Kohlstedt, Science **313** 181 (2006).
[7] T. Kimura, S. Kawamoto, I. Yamada, *et al*., Phys. Rev. B **67** 180401(R) (2003).
[8] A. S. Borovik-Romanov, Soviet Phys. JETP **11** 786 (1960).
[9] H. Grimmer, Acta. Crystallogr. A **48** 266 (1992).
[10] D. N. Astrov, Soviet Phys. JETP **11** 708 (1960).
[11] D. N. Astrov, Soviet Phys. JETP **13** 729 (1961).

[12] G. T. Rado, Phys. Rev. Lett. **6** 609 (1961).
[13] P. Borisov, A. Hochstrat, X. Chen, *et al.*, Phys. Rev. Lett. **94** 117203 (2005).
[14] C. Binek, P. Borisov, X. Chen, *et al.*, Eur. Phys. J. B **45** 197 (2005).
[15] S. A. Chambers, Surf. Sci. Rep. **39** 105 (2000).
[16] R. L. White and T. G. Phillips, J. Appl. Phys. **39** 579 (1968).
[17] G. Gorodetsky, R. M. Hornreich and S. Shtrikman, Phys. Rev. Lett. **31** 938 (1973).
[18] T. G. Worlton, R. M. Brugger and R. B. Bennion, J. Phys. Chem. Sol. **29** 435 (1968).
[19] H. Yang and R. J. Sladek, Phys. Rev. B. **32** 10 (1985).
[20] R. Hornreich and S. Shtrikman, Phys. Rev. **161** 506 (1967).
[21] J. Kushauer, W. Kleemann, J. Mattsson, *et al.*, Phys. Rev. B **49** 6346 (1994).